

Detection of Moving Targets by Passive Radar Using FM Signals on Moving Platforms

Kadir İLERİ*, Necmi Serkan TEZEL

Abstract: In this study, using FM radio signals for transmitters of opportunity, detection of moving targets by passive radar on moving platforms is investigated. Ground reflectivity is modelled as discrete patch approximation with uniform distribution in phase and Rayleigh distribution in amplitude. The target echo is modelled as Doppler shifted and delayed form of the transmit signal based on the target's angular position, range, and velocity. The clutter echoes, received by surveillance antennas, are also modelled by the superposition of Doppler shifted and delayed form of the transmit signal. Displaced Phase Center Array (DPCA) method is used for clutter rejection and moving target detection. Both matched filter and reciprocal filter are used in the pulse compression stage. The performance of the proposed method is evaluated by using an improvement factor (IF). DPCA with reciprocal filter outperforms DPCA with matched filter with the improvement value of 5,1 dB due to the reciprocal filter producing time-invariant impulse responses.

Keywords: airborne radar; displaced phase center array; ground moving target indication; passive radar; space-time adaptive processing

1 INTRODUCTION

Recently, the interest in passive radars also known as passive coherent location for surveillance purposes has increased considerably [1-8].

Target detection and localization perform with various benefits such as operating covertly, low-cost hardware setup, reduced electromagnetic pollution, and low vulnerability to electronic countermeasure due to the lack of dedicated transmitter in passive radar systems. On the other hand, the lack of the transmitter in the passive radar systems brings drawbacks such as not having control over the transmitted signal and complicated signal processing. Countless transmitters can be used as transmitters of opportunity for radio navigation, remote sensing applications, and telecommunications [3, 9-13]. Each transmitter has its own advantages such as being non-commercial, long-range coverage area, and high range resolution. The range resolution of GSM transmitter is low due to narrow band frequency [13]. On the other hand, the range resolution of DVB-T transmitter is high due to wide band frequency [3]. For long-range surveillance applications, the broadcast transmitters are the most attractive choices because of their high transmit powers. In particular, FM radio transmitters which are noncooperative and commercial stations, are the most prevalent signals for passive radar systems due to their fine trade-off between entire system development cost and performance [12]. The FM radio transmitter has long-range coverage area thanks to high transmit power. On the contrary, its range resolution is low. Many researches have been conducted for using different analogue signals such as UHF television and HF radio broadcasts for a transmitter of opportunity in passive radar applications [14-16].

Most of the passive radar systems are ground-based and stationary. Recently, passive radar systems are installed on moving platforms. In 2007, the practicability of applying passive radar to a mobile platform configuration was demonstrated with an experiment performed by using a ground vehicle [17]. In this experiment, aircraft has been successfully detected by surveillance antennas mounted on a vehicle. In the second experiment, the passive radar system mounted on an airborne platform has been tested for the first time in 2008

[18]. Since the signal of the target aircraft located in the exo-clutter region due to its high velocity, detection of moving aircrafts by ground based passive radar is based on only temporal processing. However, because of motion induced clutter spread, airborne ground moving target indication (GMTI) is based on spatial and temporal processing and exploiting the angle-Doppler relationship of clutter to reduce clutter power.

The studies on airborne passive GMTI are still at a research phase. Due to waveform instability in passive radar systems, clutter analysis, suppression, and detection performance are different from active radars and have to be investigated. In the literature, a series of airborne passive GMTI related papers are from University College London [19, 20], Research Centre of the French Air Force [21, 22], and Warsaw University of Technology [23, 24].

The main difference between active radar and passive radar is that passive radar uses existing signals in an environment for the transmitter of opportunity. The source of these signals comes from mainly civilian applications such as GSM, GPS, Wi-Fi, or radio broadcasting, and they are not proper for radar application because of waveform instability. In radar applications, a signal ambiguity function is required to stable for clutter cancellation.

To deal with waveform instability, the reciprocal filtering in passive radar has been proposed to control the sidelobes level and to mitigate the undesired properties obtained in the signal ambiguity function (AF), especially for OFDM signals [25-29]. Recently, performances of passive GMTI on moving platforms with matched filtered DPCA for different FM waveforms and clutter modelled by discrete patch approximation are investigated [30]. Similarly, the GMTI problem for passive radar on mobile platforms which is using digital video broadcast-terrestrial (DVB-T) signals for transmitter of opportunity is investigated by a processing scheme based on the cascade of the reciprocal filtering (RF) stage and the DPCA in [31].

In this study, GMTI performance of both matched filtered and reciprocal filtered based DPCA passive radar on moving platforms, which uses frequency modulated (FM) radio signal for the transmitter of opportunity, is investigated. Clutter is modelled by discrete patch approximation. For matched filtered DPCA, it is observed that some decrease and instability exist in performance due

to waveform instability. But this drawback can be removed by using the reciprocal filter instead of matched filter in the pulse compression stage, since the shape of compressed pulse obtained by the reciprocal filter is the same from batch to batch that results in perfect removal of clutter. The reciprocal filter outperforms matched filter due to the reciprocal filter producing time-invariant impulse responses in the pulse compression stage for the clutter removal with the DPCA. Besides, blind velocities, which are some particular velocities of targets which cannot be detected by the passive radar system, are analysed.

2 SIGNAL, CLUTTER, MODEL, AND DPCA PROCESSING

2.1 Reference Scenario

Let's assume that a passive radar system installed on a moving platform, which has two surveillance channels (A_0, A_1) with spatial separation d and one reference channel (A_R), uses an FM radio signal as a transmitter of opportunity (T_X). The platform moves with constant velocity (v_p) at the constant altitude (H_p) along the y -axis (see Fig. 1). The intercepted transmit signal by a reference channel is given by $s(t)$ in the baseband. $s(t)$ is called a reference signal which is assumed to be multipath free. The Doppler shift induced by platform motion can be suppressed by means of the cancellation stage [32].

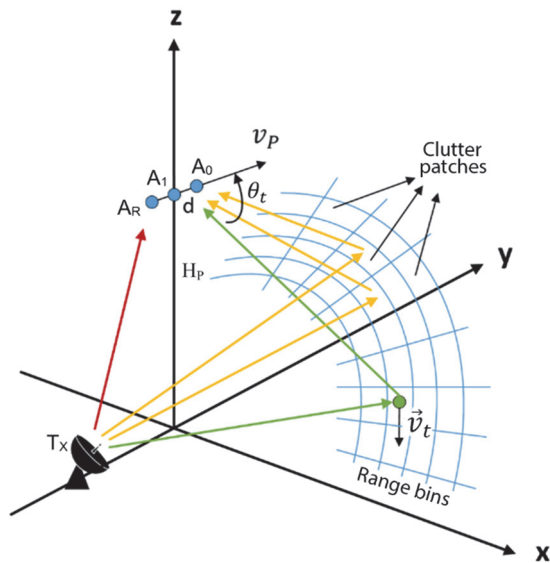


Figure 1 System geometry

The region of interest on the ground is illuminated by an FM radio transmitter. This region contains scatterer and may contain moving targets. Since we are interested in the GMTI mode of radar, detection of moving targets is our interest. Transmitted signal scattered from the ground and intercepted by surveillance channels, this signal, which is out of our interest, is called as clutter $c(t, n)$ for $n = 0, 1$.

For the clutter model, by using discrete patch approximation, the clutter is the result of scattering from many scatterers on the ground which is illuminated by a surveillance antenna beam. The amplitudes of these scatterers are assumed to be complex Gaussian distributed. It is also assumed that clutter is stationary or does not have any internal clutter motion (ICM).

2.2 Signal Model

The clutter can be given by:

$$c(t, n) = \sum_{m=1}^{N_a} \sum_{k=1}^{N_r} A_{mk} s(t - R_k / c_0) e^{i \left(\frac{2\pi}{\lambda} \right) \cos(\theta_m) (v_p t + nd)} \quad (1)$$

where $n = 0, 1$ is surveillance channel index and channel index decreases along platform velocity direction, N_a and N_r are number of scatterers along with angular and range directions respectively, $\theta_m = \left(\frac{m\pi}{M} \right) - \frac{\pi}{2}$ is m -th angular

location of scatterers, this angle is defined as between platform velocity and direction from platform to the m -th scatterer, ΔR_k is the k -th bistatic range, v_p is the velocity of aircraft, λ is the wavelength, c_0 is the velocity of light and A_{mk} is complex amplitude of scatterer located at m -th angular and k -th bistatic range location.

Target signal can be written as:

$$s(t, n) = A_t s \left(t - \frac{R_t}{c_0} \right) e^{i \left(\frac{2\pi}{\lambda} \right) \cos(\theta_t) nd} e^{i 2\pi f_d t} \quad (2)$$

where A_t is the amplitude of the signal, which is governed by the radar range equation, θ_t is the angle between platform velocity and direction from platform to target, R_t and f_d are bistatic range and bistatic Doppler of the target, respectively.

Bistatic Doppler f_d can be written as:

$$f_d = \frac{v_p}{\lambda} \cos \theta_t + \frac{\vec{v}_t \cdot (\hat{u}_{tT} + \hat{u}_{tR})}{\lambda} \quad (3)$$

where \vec{v}_t is target velocity vector, \hat{u}_{tT} and \hat{u}_{tR} are unit vectors from target to transmitter and from target to receiver, respectively. The received signal can be written as:

$$r = s + c + n_w \quad (4)$$

where n_w is statistical independent identical distributed additive complex Gaussian white noise whose power is $E[n_w^2] = \sigma^2$. The received signal is discretized by an analog-digital converter (ADC) as:

$$rd(l, n) = r(lT_s, n) \quad (5)$$

where T_s is the sampling period of the ADC and this signal is segmented as:

$$u(l, m, n) = rd(l + (m-1)L, n) \quad (6)$$

where $l, 1 \leq l \leq 2L$ is range samples also called as fast time samples, $m, 0 \leq m \leq M-1$ is segment number also called as slow time samples or batch number. This

segmented signal is passed through the pulse compressing stage as:

$$x(l, m, n) = \sum_{b=0}^{L-1} u(l-b, m, n) h_m(b) \quad (7)$$

where $h_m(l), 0 \leq l \leq L-1$ pulse compressing filter for each segment of the signal, $h_m(l)$ is usually chosen as a matched filter to maximize signal to noise ratio as:

$$h_m^{MF}(l) = ref_m^*(L-1-l) \quad (8)$$

or, $h_m(l)$ is chosen as a reciprocal filter to avoid fluctuations of the compressed pulse from batch to batch as [32]:

$$h_m^{RF}(l) = IDFT(1 / (DFT(ref_m(l))) \quad (9)$$

where $ref_m(l)$ is sampled and segmented version of the reference signal received by reference antenna as:

$$ref_m(l) = s(lT_s + mLT_s), 0 \leq l \leq L-1, 0 \leq m \leq M-1 \quad (10)$$

DFT and $IDFT$ are discrete Fourier transform and inverse discrete Fourier transform, respectively. In Eq. (9), DFT and $IDFT$ are performed over l .

The reference signal has Doppler shift because of platform motion and may have multipath signal. The Doppler shift in reference signal can be suppressed by the cancellation process [32]. Multipath signal in reference signal can be removed by constant modules algorithm [33].

2.3 DPCA Processing

The clutter effects which are caused by the platform motion appear in passive GMTI. These clutter effects affect the target detection in a negative way. The DCPA method is used to suppress these clutter effects for proper target detection in passive GMTI [23, 24].

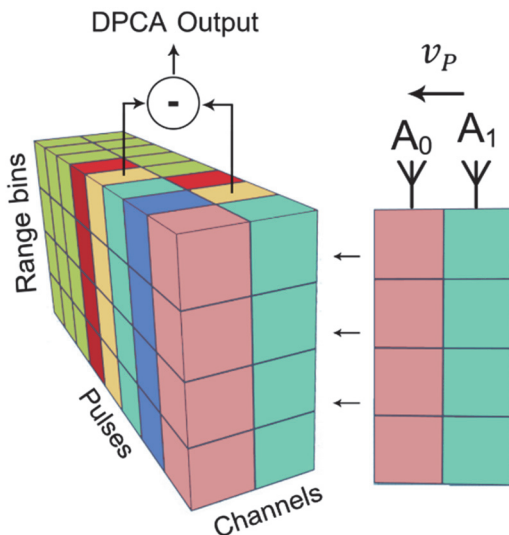


Figure 2 Demonstration of the DPCA processing

The DCPA method is performed by subtracting the received echoes by the two surveillance channels as shown in Fig. 2. The channels are mounted in side-looking condition and their phase centres occupy the same spatial position at different points of time.

DPCA processing is performed as:

$$y(l, m) = x(l, m, 1) - x(l, m - K, 0) \quad (11)$$

where $K = \frac{d}{v_p T_s L}$. If K is not integer, we can apply

interpolation to evaluate second term of Eq. (11) or apply the approximation given in [31]. This processing in Eq. (11) causes notch filters located on $f_n = \frac{mv_p}{d}, m = 0, \mp 1, \mp 2, \dots$. After DPCA processing, DFT is applied to signal y over slow time dimension and M

frequency bins are formed with $f_u = \frac{1}{LT_s}$ unambiguous

Doppler as:

$$Y(l, k) = \sum_{m=0}^{M-1} y(l, m) e^{-i2\pi km/M} \quad (12)$$

where M is the total number of batches collected during the coherent processing interval (CPI).

The performance of the DPCA processing is evaluated by using IF as a metric over Doppler frequency of interest given by:

$$IF = \frac{SCNR_{out}}{SCNR_{in}} \quad (13)$$

where $SCNR_{in}$ is the signal to clutter plus noise ratio at the input before DPCA processing is performed, and is given by:

$$SCNR_{in}(l_0, p) = \frac{E \left[|X_s(l_0, p_0; l_0, p_0)|^2 \right]}{E \left[|X_c(l_0, p_0)|^2 \right] + \sigma^2 \sum_{m=0}^{M-1} \sum_{b=0}^{L-1} |h_m(b)|^2} \quad (14)$$

where X_s is FFT of the target signal whose bistatic range bin l_0 and bistatic Doppler bin p_0 at generic bistatic range bin l and generic Doppler bin p before DPCA is given by:

$$X_s(l, p; l_0, p_0) = \sum_{m=0}^{M-1} x_s(l, m, 0) e^{-i2\pi pm/M} \quad (15)$$

and X_c is FFT of the clutter at bistatic range bin l_0 and bistatic Doppler bin p_0 before DPCA given by:

$$X_c(l_0, p_0) = \sum_{m=0}^{M-1} x_c(l, m, 0) e^{-i2\pi pm/M} \quad (16)$$

$SCNR_{out}$, that is signal to clutter plus noise ratio at the output after DPCA processing, can be calculated as:

$$SCNR_{out}(l_0, p_0) = \frac{E\left[|Y_s(l_0, p_0; l_0, p_0)|^2\right]}{E\left[|Y_c(l_0, p_0)|^2\right] + 2\sigma^2 \sum_{m=0}^{M-1} \sum_{b=0}^{L-1} |h_m(b)|^2} \quad (17)$$

where Y_s is FFT of the target signal whose bistatic range bin l_0 and bistatic Doppler bin p_0 at generic bistatic range bin l and generic Doppler bin p after DPCA and is given by:

$$Y_s(l, p; l_0, p_0) = \sum_{m=0}^{M-1} y_s(l, m) e^{-i2\pi p m / M} \quad (18)$$

Y_c is FFT of the clutter at bistatic range bin l_0 and bistatic Doppler bin p_0 after DPCA and is given by:

$$Y_c(l_0, p_0) = \sum_{m=0}^{M-1} y_c(l, m) e^{-i2\pi p m / M} \quad (19)$$

where first and second terms in Eq. (14) and Eq. (17) are clutter power and white noise power, respectively. The white noise power is calculated based on statistical independent and identically distributed assumption of white noise.

Substituting Eq. (17) and Eq. (14) into Eq. (13), one gets IF in Eq. (11) as:

$$\frac{E\left[|X_c(l_0, p_0)|^2\right] + \sigma^2 \sum_{m=0}^{M-1} \sum_{b=0}^{L-1} |h_m(b)|^2}{E\left[|Y_c(l_0, p_0)|^2\right] + 2\sigma^2 \sum_{m=0}^{M-1} \sum_{b=0}^{L-1} |h_m(b)|^2} \cdot \frac{E\left[|Y_s(l_0, p_0; l_0, p_0)|^2\right]}{E\left[|X_s(l_0, p_0; l_0, p_0)|^2\right]} \quad (20)$$

IF depends on CNR at the input that is given by:

$$CNR = \frac{E\left[|c(t, 0)|^2\right]}{\sigma^2} \quad (21)$$

Since clutter on each bistatic range and angular direction is assumed to be statistically independent, Eq. (21) can be calculated as:

$$CNR = \frac{E\left[|s(t)|^2\right] \sum_{m=1}^{N_a} \sum_{k=1}^{N_r} |A_{mk}|^2}{\sigma^2} \quad (22)$$

Once the range and Doppler shift of the target are obtained from single platform, the exact location of the target in 3D coordinate system can be extracted by triangulation [11].

3 RESULTS AND DISCUSSION

In this study, detection of moving targets by passive radar using FM radio signals on moving platforms is investigated. The proposed DPCA method using both the

matched filter and the reciprocal filter is applied and improvement factors are obtained. FM waveform with the duration of 1,4 s and sampled at 200 kHz is used as an illumination opportunity which gives about 2km range resolution. The common parameters for simulations are the platform velocity $v_p = 500$ m/s, wavelength $\lambda = 3$ m, CNR 40 dB, batch size $L = 100$, batch number $M = 93$, the distance between antennas $d = 0,5$ m, which should be less than $\lambda/2=1,5$ m. Ground clutter is modelled by scattering from the ground with $N_r = 100$ and $N_a = 30$ complex Gaussian distributed scatterers along with range and angle directions, respectively.

We compare the performances of the matched filter and the reciprocal filter for DPCA. Range-Doppler maps are obtained before and after DPCA processing for both matched filter and reciprocal filter.

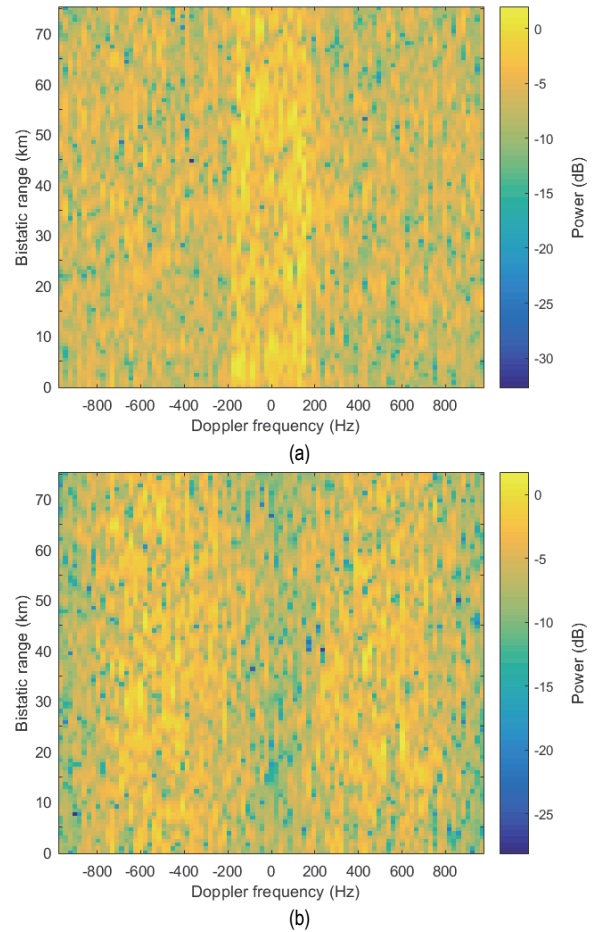


Figure 3 Range-Doppler map for matched filter including clutter echoes only: (a) before DPCA processing; (b) after DPCA processing

As seen in Fig. 3a, strong clutter echoes occur at $[-166 \text{ Hz}, 166 \text{ Hz}]$ Doppler interval (endo-clutter region) for entire range bins. This Doppler interval value depends on the wavelength λ and platform velocity v_p . The detection of slowly moving targets (whose Doppler shift is between $\left[-\frac{v_p}{\lambda}, \frac{v_p}{\lambda}\right]$) is masked due to these strong clutter echoes.

Besides, clutter echoes appear at higher Doppler frequencies (exo-clutter region) because of the uncontrollable characteristics of the employed signal [28].

After DPCA processing, the contributions of strong clutter echoes decreased by an average of 10 dB as seen in

Fig. 3b. This decrease is not sufficient for slowly moving target detection. In addition, the clutter echoes at higher Doppler frequencies increased by an average of 5 dB. This increase makes the target detection difficult.

As seen in Fig. 4a, strong clutter echoes occur at $[-166 \text{ Hz}, 166 \text{ Hz}]$ Doppler interval for entire range bins which masks the slowly moving targets. After DPCA processing, all the contributions of strong clutter echoes are removed as seen in Fig. 4b. Furthermore, the clutter echoes at higher Doppler frequencies are completely removed. However, as a result of the DPCA processing, only residues from the noise in the receiving system remained. These residues are too small to interfere with target detection.

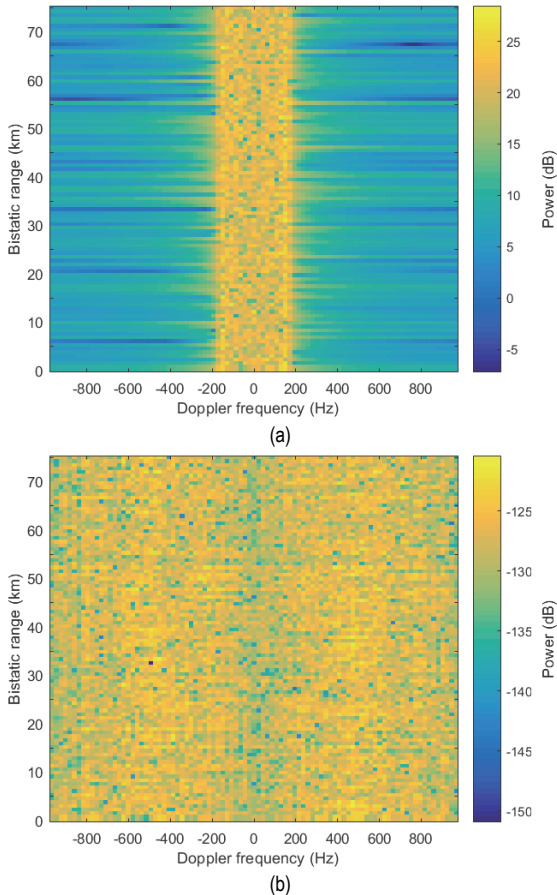


Figure 4 Range-Doppler map for reciprocal filter including clutter echoes only: (a) before DPCA processing; (b) after DPCA processing

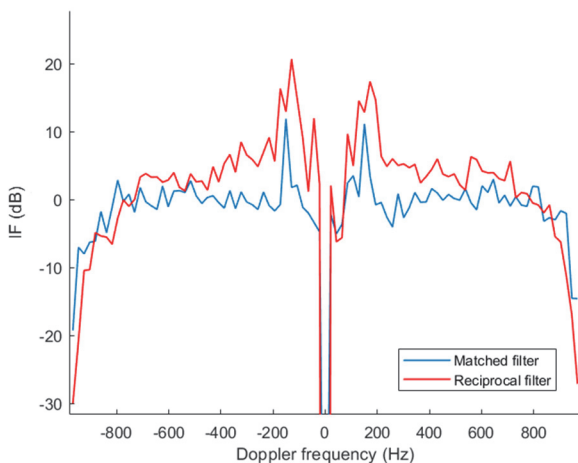


Figure 5 IF with respect to bistatic Doppler of DPCA for matched filter and reciprocal filter

The obtained IF of DPCA for matched filter and reciprocal filter by using Eq. (20) is depicted in Fig. 5. The reciprocal filter outperforms matched filter with the improvement value of 5,1dB. The reason for the difference between matched filter and reciprocal filter results is due to waveform instability. While the matched filter produces time-variant impulse responses in the pulse compression stage for the clutter removal with the DPCA, the reciprocal filter produces time-invariant impulse responses. This difference is not negligible because of affecting target detection as seen in Fig. 6, Fig. 7, Fig. 8, and Fig. 9.

3.1 Results for Targets at Different Velocities and Ranges

We compare the performances of the DPCA with matched filter and the DPCA with reciprocal filter for two targets at different velocities and ranges (assumed in broadside direction). One of the targets (Target₁) has a velocity of 131 m/s and is at a range of 67,5 km, the other (Target₂) has a velocity of 1977 m/s and is at a range of 37,5 km.

For the Target₁, target detection is failed before and after DPCA with matched filter due to strong clutter echoes as seen in Fig. 6.

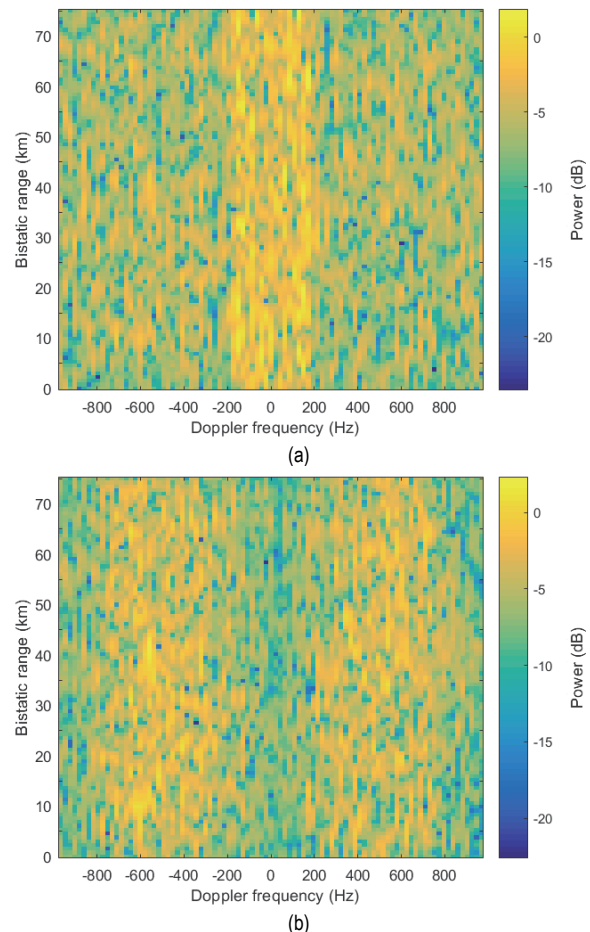


Figure 6 Range-Doppler map for matched filter including target (Target₁), clutter, and noise: (a) before DPCA processing; (b) after DPCA processing

As seen in Fig. 7a, target detection is failed before DPCA with reciprocal filter due to strong clutter echoes. On the contrary, target detection is successful after DPCA with reciprocal filter thanks to perfect clutter removal as seen in Fig. 7b.

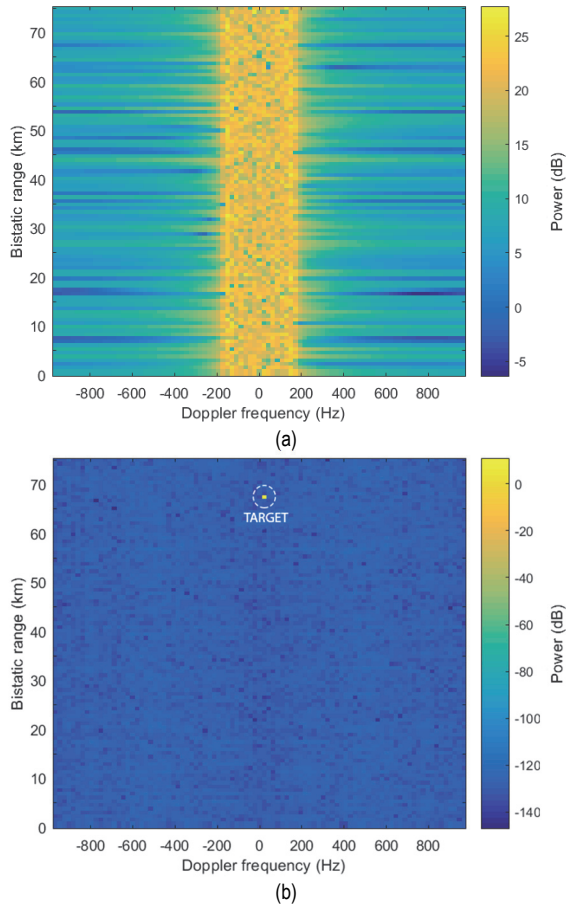


Figure 7 Range-Doppler map for reciprocal filter including target (Target₁), clutter, and noise: (a) before DPCA processing; (b) after DPCA processing

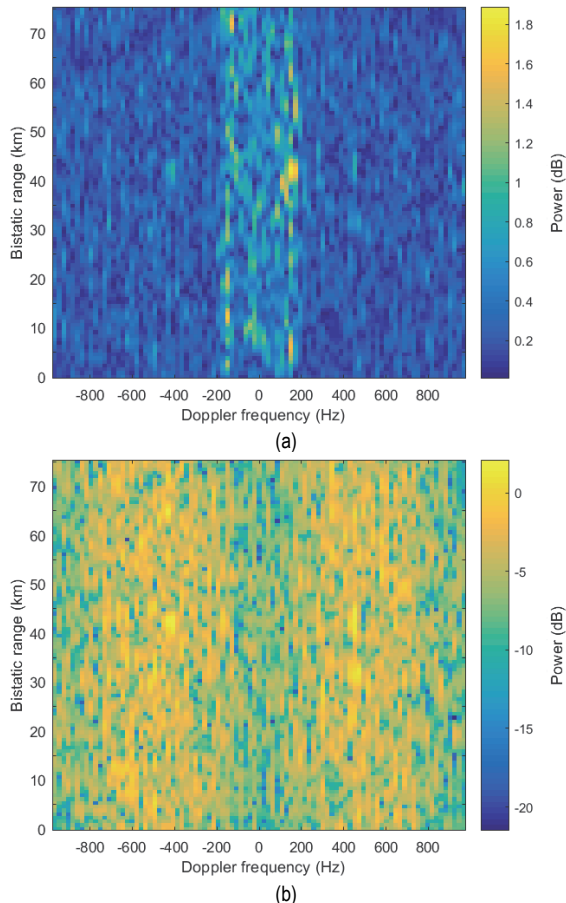


Figure 8 Range-Doppler map for matched filter including target (Target₂), clutter, and noise: (a) before DPCA processing; (b) after DPCA processing

For the Target₂, target detection is failed before and after DPCA with matched filter due to clutter echoes as seen in Fig. 8.

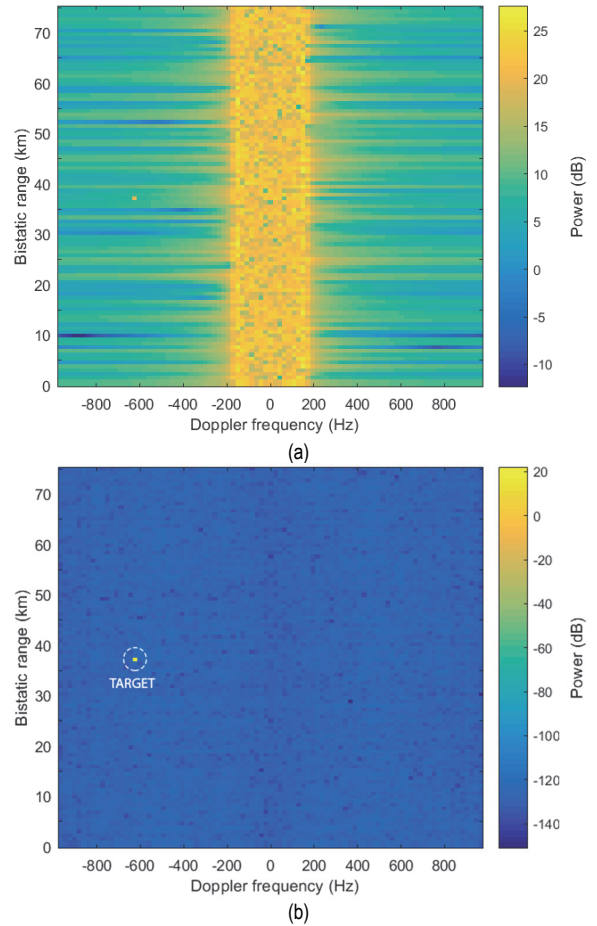


Figure 9 Range-Doppler map for reciprocal filter including target (Target₂), clutter, and noise: (a) before DPCA processing; (b) after DPCA processing

As seen in Fig. 9a, target is relatively detectable before DPCA with reciprocal filter due to being outside of the Doppler interval of slowly moving target. But this is not enough for perfect target detection. On the contrary, target detection is successful after DPCA with reciprocal filter thanks to perfect clutter removal as seen in Fig. 9b.

3.2 Analysis of Blind Velocities

The passive radar system cannot detect the targets which have some particular velocities. These velocities are called blind velocities and occur at f_n Doppler shift values of target (see Section 2.3).

Blind velocities depend on T_{dpca} time which is given as follows:

$$T_{dpca} = KT_s \tag{23}$$

For the simulated scenario, $d = 0,5$ m and $v_p = 500$ m/s, $K = 2$, $T_s = 0,5$ ms and $T_{dpca} = 1$ ms. Therefore, blind velocities occur at $f_n = m \cdot 1000$ ($m = 0, \mp 1, \mp 2, \dots$) which can be clearly seen in Fig. 10.

The number of blind velocities increases as the T_{dpca} time increases. On the other hand, increasing the T_{dpca} time makes it possible to detect very slow moving targets

with a low Doppler shift. The T_{dpca} time should be adjusted considering these effects on blind velocities.

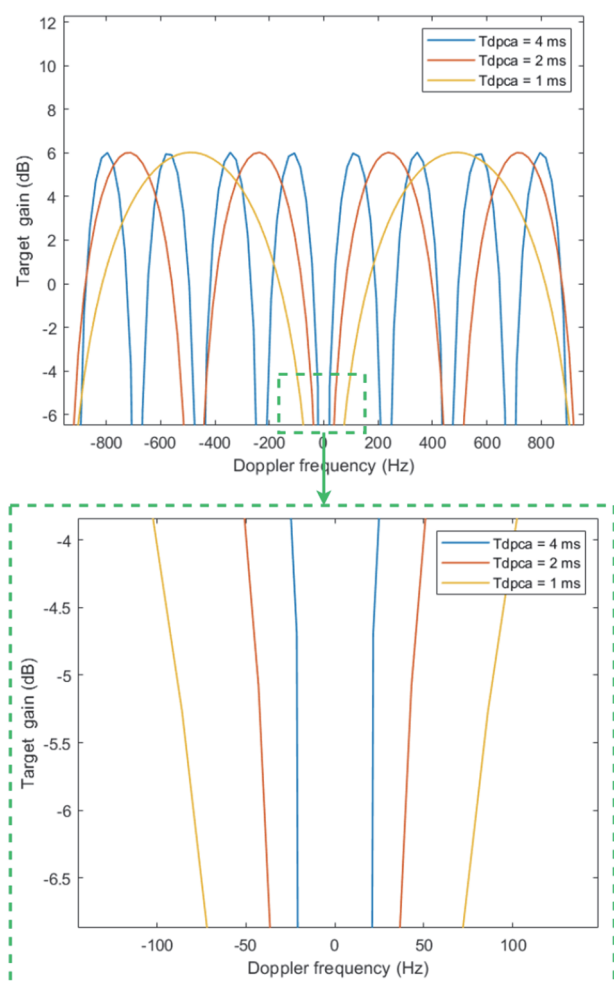


Figure 10 Blind velocities for different T_{dpca} times

4 CONCLUSION

In this study, the GMTI performance of the passive radar using FM waveform as an illumination opportunity on moving platforms based on DPCA processing using both matched filter and reciprocal filter on range compression stage is evaluated by using IF as a metric. Although FM signal provides poor range resolution because of small bandwidth but high transmit power, it can be used in naval application such as detection of ships by secret operation. The matched filter is the filter that maximizes the signal to noise ratio in the pulse compression stage but has an unstable response from batch to batch; on the other hand reciprocal filter provides stable compressed pulse from batch to batch but does not maximize signal to noise ratio in pulse compression stage.

Range-Doppler maps are obtained for targets at different velocities and ranges to analyse exo-clutter and endo-clutter target detection performance of passive radar system. DPCA with reciprocal filter outperforms DPCA with matched filter due to the reciprocal filter producing time-invariant impulse responses in the pulse compression stage. Moreover, blind velocities, which are some particular velocities of targets and cannot be detected by the passive radar system, are investigated.

5 REFERENCES

- [1] Howland, P. (2005). Editorial: Passive radar systems. *IEEE Proceedings on Radar, Sonar and Navigation*, 152(3), 105-106. <https://doi.org/10.1049/ip-rsn:20059064>
- [2] Blasone, G. P., Colone, F., Lombardo, P., Wojacek, P., & Cristallini, D. (2020). Passive Radar DPCA Schemes with Adaptive Channel Calibration. *IEEE Transactions on Aerospace and Electronic Systems*, 56(5), 4014-4034. <https://doi.org/10.1109/TAES.2020.2987478>
- [3] Plotka, M., Malanowski, M., Samczyński, P., Kulpa, K., & Abratkiewicz, K. (2020). Passive Bistatic Radar Based on VHF DVB-T Signal. *2020 IEEE International Radar Conference (RADAR)*, 596-600. <https://doi.org/10.1109/RADAR42522.2020.9114859>
- [4] Pisciotto, I., Cristallini, D., Schell, J., & Seidel, V. (2018). Passive ISAR for maritime Target Imaging: Experimental results. *Proceedings International Radar Symposium, 2018* (June). <https://doi.org/10.23919/IRS.2018.8448039>
- [5] Kuschel, H., Heckenbach, J., & Ummenhofer, M. (2017). Passive radar collision warning system PARASOL. *IEEE Aerospace and Electronic Systems Magazine*, 32(2). <https://doi.org/10.1109/MAES.2017.150267>
- [6] Blasone, G. P., Colone, F., Lombardo, P., Wojacek, P., & Cristallini, D. (2019). A two-stage approach for direct signal and clutter cancellation in passive radar on moving platforms. *2019 IEEE Radar Conference*. <https://doi.org/10.1109/RADAR.2019.8835704>
- [7] Palmer, J., Ummenhofer, M., Summers, A., Bournaka, G., Palumbo, S., & Cristallini, D. (2017). Receiver platform motion compensation in passive radar, IET Radar. *Sonar and Navigation*, 11(6), 922-931. <https://doi.org/10.1049/iet-rsn.2016.0516>
- [8] Makhoul, E., Baumgartner, S. V., Jager, M., & Broquetas, A. (2015). Multichannel SAR-GMTI in Maritime Scenarios with F-SAR and TerraSAR-X Sensors. *IEEE Journal of Selected Topics in Applied Earth Observations and Remote Sensing*, 8(11), 5052-5067. <https://doi.org/10.1109/JSTARS.2015.2438898>
- [9] Basyigit, I. B. & Dogan, H. (2020). Troubleshooting of Handover Problems in 900 MHz for Speech Quality. *Wireless Personal Communications*, 114, 1833-1845. <https://doi.org/10.1007/s11277-020-07451-7>
- [10] Griffiths, H. D. & Baker, C. V. (2005). Passive coherent location radar systems. Part 1: Performance prediction. *IEEE Proceedings on Radar, Sonar and Navigation*, 152(3), 153-159. <https://doi.org/10.1049/ip-rsn:20045082>
- [11] Lombardo, P. & Colone, F. (2012). Advanced Processing Methods for Passive Bistatic Radar Systems, Principles of Modern Radar: Advanced Radar Techniques. USA: SciTech Publishing. <https://doi.org/10.1049/SBRA020E>
- [12] Howland, P. E., Maksimiuk, D., & Reitsma, G., (2005). FM radio based bistatic radar. *IEEE Proceedings on Radar, Sonar and Navigation*, 152(3), 107-115. <https://doi.org/10.1049/ip-rsn:20045077>
- [13] Basyigit, I. (2021). Empirical path loss models for 5G wireless sensor network in coastal pebble/sand environments. *International Journal of Microwave and Wireless Technologies*, 1-10. <https://doi.org/10.1017/S1759078721001574>
- [14] Griffiths, H. D. & Long, N. R. (1986). Television based bistatic radar. *IEEE Proceedings on Communications, Radar and Signal Processing*, 133(7), 649-657. <https://doi.org/10.1049/ip-f-1.1986.0104>
- [15] Howland, P. E. (1999). Target tracking using television-based bistatic radar. *IEEE Proceedings on Radar, Sonar and Navigation*, 146(3), 166-174. <https://doi.org/10.1049/ip-rsn:19990322>
- [16] Fabrizio, G., Colone, F., Lombardo, P., & Farina, A. (2009). Adaptive beam forming for high frequency over-the-horizon

- passive radar. *IET Radar, Sonar and Navigation*, 3(4), 384-405. <https://doi.org/10.1049/iet-rsn.2008.0159>
- [17] Dawidowicz, B. & Kulpa, K. (2008). Experimental results from PCL radar on moving platform. *Proceedings of the International Radar Symposium 2008*, 305-308. <https://doi.org/10.1109/IRS.2008.4585777>
- [18] Kulpa, K., Malanowski, M., Misiurewicz, J., Mordzonek, M., Samczynski, P., & Smolarczyk, M. (2008). Airborne PCL radar: the concept and primary result. *Proceedings of the Military Radar Conference 2008*.
- [19] Brown, J., Woodbridge, K., Stove, A., & Watts, S. (2010). Air target detection using airborne passive bistatic radar. *Electronics Letters*, 46(20), 1396-1397. <https://doi.org/10.1049/EL.2010.1732>
- [20] Brown, J., Woodbridge K., Griffiths, H., Stove, A., & Watts, S. (2012). Passive bistatic radar experiments from an airborne platform. *IEEE Aerospace and Electronic Systems Magazine*, 27(11), 50-55. <https://doi.org/10.1109/MAES.2012.6380826>
- [21] Raout, J., Neyt, X., & Rischette, P. (2007). Bistatic STAP using DVB-T illuminators of opportunity. *IET International Conference on Radar Systems*. <https://doi.org/10.1049/cp:20070670>
- [22] Raout, J., Santori, A., & Moreau, E. (2010). Space-time clutter rejection and target passive detection using the APES method. *IET Signal Processing*, 4(3), 298-304. <https://doi.org/10.1049/iet-spr.2009.0067>
- [23] Dawidowicz, B., Samczynski, P., Malanowski, M., Misiurewicz, J., & Kulpa, K. (2012). Detection of moving targets with multichannel airborne passive radar. *IEEE Aerospace and Electronic Systems Magazine*, 27(11). <https://doi.org/10.1109/MAES.2012.6380825>
- [24] Dawidowicz, B., Kulpa, K., Malanowski, M., Misiurewicz, J., Samczynski, P., & Smolarczyk, M. (2012). DPCA detection of moving targets in airborne passive radar. *IEEE Transactions on Aerospace and Electronic Systems*, 48(3), 1347-1357. <https://doi.org/10.1109/TAES.2012.6178066>
- [25] Glende, M. (2006). PCL-Signal-Processing for Sidelobe Reduction in Case of Periodical Illuminator Signals. *International Radar Symposium*. <https://doi.org/10.1109/IRS.2006.4338042>
- [26] Searle, S., Palmer, J., Davis, L., O'Hagan, D., & Ummenhofer, M. (2014). Evaluation of the ambiguity function for passive radar with OFDM transmissions. *IEEE Radar Conference*, 1040-1045. <https://doi.org/10.1109/RADAR.2014.6875747>
- [27] Palmer, J., Harms, H., Searle, S., & Davis, L. (2016). DVB-T Passive Radar Signal Processing. *IEEE Transactions on Signal Processing*, 61(8), 2116-2126. <https://doi.org/10.1109/TSP.2012.2236324>
- [28] Gassier, G., Chabriel, G., Barrère, J., Briolle, F., & Jauffret, C. (2016). A Unifying Approach for Disturbance Cancellation and Target Detection in Passive Radar Using OFDM. *IEEE Transactions on Signal Processing*, 64(22), 5959-5971. <https://doi.org/10.1109/TSP.2016.2600511>
- [29] Chabriel, G. & Barrere, J. (2017). Adaptive Target Detection Techniques for OFDM-based Passive Radar Exploiting Spatial Diversity. *IEEE Transactions on Signal Processing*, 65(22), 5873-5884. <https://doi.org/10.1109/TSP.2017.2742980>
- [30] Tezel, N. S., Colone, F., & Lombardo, P. (2016). Ground Moving Target Detection Performance of Displaced Phase Center Array Method for Airborne Passive Radar. *4th International Conference on Advanced Technology and Science*.
- [31] Wojaczek, P., Colone F., Cristallini, D., & Lombardo, P. (2019). Reciprocal-Filter-Based STAP for Passive Radar on Moving Platforms. *IEEE Transactions on Aerospace and Electronic Systems*, 55(2), 967-988. <https://doi.org/10.1109/TAES.2018.2867688>
- [32] Colone, F., Palmarini, C., Martelli, T., & Tilli, E. (2016). Sliding extensive cancellation algorithm for disturbance removal in passive radar. *IEEE Transactions on Aerospace and Electronic Systems*, 52(3), 1309-1326. <https://doi.org/10.1109/TAES.2016.150477>
- [33] Colone, F., Cardinali, R., Lombardo, P., Crognale, O., Cosmi, A., Lauri, A., & Bucciarelli, T. (2009). Space-time constant modulus algorithm for multipath removal on the reference signal exploited by passive bistatic radar. *IET Radar, Sonar & Navigation*, 3, 253-264. <https://doi.org/10.1049/iet-rsn:20080102>

Contact information:

Kadir İLERİ, PhD
(Corresponding author)
Department of Electrical and Electronics Engineering,
Faculty of Engineering, Office 114, Karabuk University,
78050 Karabuk, Turkey
E-mail: kadirileri@karabuk.edu.tr

Necmi Serkan TEZEL, PhD, Professor
Department of Electrical and Electronics Engineering
Faculty of Engineering, Office 128, Karabuk University,
78050 Karabuk, Turkey
E-mail: nstezel@karabuk.edu.tr